

# Multi-Scale Modeling of Composites with Surrogate and Uncertainty in Residual Velocity for High-Speed Impacts

Minhyung Lee

*School of Mechanical and Aerospace Engineering  
Sejong University, Seoul, South Korea  
mlee@sejong.ac.kr*

Nam H. Kim

*Department of Mechanical and Aerospace Engineering  
College of Engineering, University of Florida, USA*

Received 18 August 2017  
Revised 21 December 2017  
Accepted 22 December 2017  
Published 2 February 2018

The bullet impact onto a composite plate has been investigated both numerically and experimentally. The main purpose is to numerically identify the range of uncertainty shown in the residual velocities from the high-speed impact test data. The simulation is based on the multi-scale modeling for composites. The experimental results presented here include the tensile tests of composite specimen to identify the range of failure strains and mainly the ballistic shot test onto a laminated plate to measure the residual velocities with especial interests in the range of uncertainty. All test data have been compared with numerical predictions and the scattered test data are reasonably well captured with simulations.

*Keywords:* Composite plate; ballistic impact; multi-scale modeling; residual velocity; uncertainty.

## 1. Introduction

Due to high stiffness, improved strength and toughness, composite materials draw strong attention in many engineering applications. Specifically, they are applied to protect threats such as fragments and bullets. Previous attempts to analyze the bullet impact onto composite plates were mainly to predict the residual velocity (the velocity after passing through the plate) as a function of impact velocity [Sun and Potty, 1996; Chocron *et al.*, 1997; Raguraman *et al.*, 2010] or the critical ballistic velocity (V50), defined as the velocity having at least 50% of change perforating a particular thickness of material plate [Ryan *et al.*, 2008; Ryan and Christiaansen, 2010; Grujicic *et al.*, 2013]. Some studies were conducted for the application of the composites to the hypervelocity impact problems [Katz *et al.*, 2008; Lee, 2014].

A progressive failure model has been continuously updated for the low velocity impacts onto composite armors [Bandaru and Ahmad, 2015].

On the other hand, the inherent characteristic of composite materials is showing a relatively significant irregularity in mechanical properties. This leads to uncertainty in structural performance. The uncertainty propagation from local to global properties in composite structures was studied theoretically [Antonio and Hoffbauer, 2008]. In the ballistic area, one important parameter is the residual velocity. These data show a scatter nature even for metal plates, and become worse for the composite plates. Hence, the design group starts to request the uncertainty data, rather than just single data of residual velocity.

As part of the activities in uncertainty identification, a series of study has been conducted in this work, which includes the tensile lab test, the bullet impact field test and numerical simulations. First, a major source of uncertainty is identified by a series of the tensile test. It was anticipated that all the combined material irregularity will be eventually revealed by the range of failure strain, which is from the macroscopic point of view. Second, high-speed shot test has been conducted and the residual velocities are measured. A sophisticated handling of the test has been made to eliminate the intrusion of possible error sources. Finally, numerical impact simulations are carried out to predict the range of uncertainty shown in the ballistic field tests.

It has been known that there are several failure mechanics. The dominant failure mechanisms considered in this work are the fiber fracture and the matrix–fiber debonding. In general, this is the case for the high-speed impact event. Some analytical models consider only the fiber breakage to predict the residual velocity after plate perforation. Their results quite match well with the experimental data [Cunniff, 1992; Chocron *et al.*, 1997]. Delamination is usually assumed to result from excessive thickness tensile stresses or strains and/or from excessive shear stresses or strains in the matrix material [Hayhurst *et al.*, 1999]. We believe that this mechanics has a minimum effect on the ballistic impact event [Naik *et al.*, 2006]. However, it could be investigated in the future study. The failure models are different in their formulation of the criteria to catch the onset of damage. After failure initiation, the failed material stiffness and strength are modified. Some works assume that a lamina behaves in an ideally brittle manner such that the stiffness abruptly reduced to zero [Williams and Vaziri, 2001], and others consider the gradual degradation with an inclusion of damage factor [Johnson and Cook, 1985].

Material test has been performed for a unidirectional composite product to find the relevant properties to be used as validation cases, and they have been described in Shang *et al.* [2014]. Some results are also used here for a further validation of the current numerical modeling. We believe that the uncertainty shown in each ply level of the meso-scale will naturally propagate into the laminates of the macro-scale causing a scatter in the ballistic performance. The present study is to apply the integrated surrogate model to the case of high-speed impact onto a composite

plate. To do this, the nonlinear finite element code, ABAQUS was used to generate a surrogate model ready to be included into any material subroutine. As a testbed, LS-DYNA3D is adopted. It will be more versatile if an in-house code is available since the data interface will be more manageable compared to the commercial code.

## 2. High-Speed Impact Test

### 2.1. Configuration

Laminated plates consisted of four and eight plies were prepared. Four plies are two in the longitudinal direction and two in the transverse direction in a 0/90/90/0 sequence. The plate dimension is 600 mm  $\times$  300 mm. The average thickness is 3.6 mm for four plies and 7.2 mm for eight plies. Fiber volume content for glass fiber-reinforced laminates is 56.3% which is an average value determined with the inspection of three specimens. The constituents of the composite material are *E*-glass fiber and epoxy resin. Their elastic properties are listed in Table 1. Basically, the same materials are used for the preparation of laminates with the tensile test specimen.

Three plates are prepared for each four and eight plies. Then, 6 shots are performed onto each plate as shown in Fig. 1, resulting in a total of 18 shots (Table 2).

Table 1. Elastic properties of fiber and matrix.

Elastic properties	Stiffness (MPa)	Poisson's ratio
<i>E</i> -glass	81,000	0.22
Epoxy	3,000	0.398



(a) Four plies

(b) Eight plies

Fig. 1. Images of fiber-reinforced composites perforated by 17 grain FSP.

Table 2. Summary of ballistic test.

Projectile	Composite plates No. of plies	Plate thickness (mm)	No. of plates	Total shots
17 grain FSP	4	3.6	3	18
	8	7.2	3	18

The main objective of the current work is not to measure the residual velocity as a function of impact velocity, but to measure the range of scatter in the residual velocity. Hence, a special effort was made to make those 18 shots done at the same condition as possible as we can. For this, extra shots were actually conducted for calibration and to guarantee a solid measurement in the residual velocity. This includes that the impact velocity is larger than the ballistic limit velocity (so-called V50).

As shown in Fig. 1, the recovered plates reveal that for such a high-speed impact, the deformation and damage zone are confined to the vicinity of impact location. This confirms no interference between the shots. One of the reasons for making six shots on the same plate is to minimize the property variation between the plates. At the same time, three plates are used to include some (if any) variations between the plates. This is aimed to cover the real situation for mass production stage of composite plates. The chosen bullet for the current test is 17 grain fragmenting simulating projectile (FSP). Because of its shape, it shows more straightness after

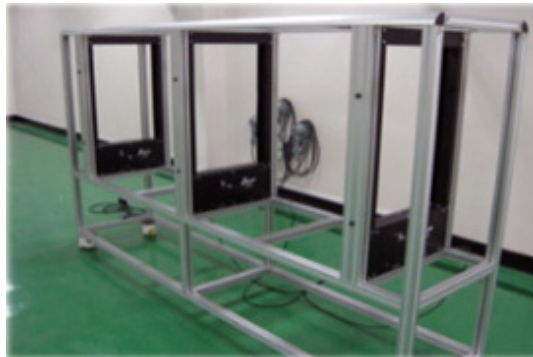


Fig. 2. Shot screens (two front and two back) to measure the impact and residual velocities.

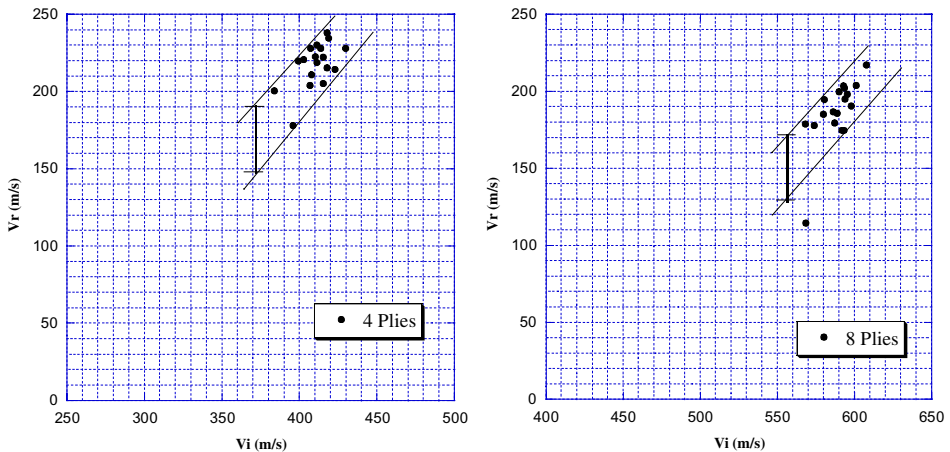


Fig. 3. The impact and residual velocity data indicating a scattered feature.

penetration of composites, thus a certain source caused by a projectile (impact angle or yaw) of the measurement error could be further eliminated. As shown in Fig. 2, four screens (two before the test area and two after the test area) are placed by standards in the line of fire at the distances and connected to the time-interval measurement equipment to measure the impact velocity and the residual velocity.

**2.2. Residual velocity and error bound**

Figure 3 shows the impact velocity versus the measured residual velocity for four plies and eight plies plates. Even though we tried to maintain the impact velocity constant for all 18 shots, there are some variations. This may not be an issue because it is natural for every firing test. This is why the high-speed dynamic impact test is expensive and not easy to make a perfect case. And this is why we need the

Table 3. Ballistic test results.

Shot No.	Impact velocity $V_i$ (m/s)	Residual velocity $V_r$ (m/s)
(a) Four plies plate (12 out of 18 shots)		
5	406.7	203.8
6	407.1	227.8
7	407.7	210.7
8	410.2	222.5
9	411.3	218.7
10	411.4	230.2
11	413.8	227.9
12	415.2	205.0
13	415.5	222.1
14	417.8	215.3
15	417.9	238.0
16	418.8	234.5
Range	406.7–418.8	203.8–238.0
Average	412.8	221.4
Uncertainty	-1.45 ~ (+)1.48%	-7.95–7.50%
(b) Eight plies plate (10 out of 18 shots)		
6	586.2	186.6
7	587.3	179.4
8	588.7	185.7
9	590.1	199.5
10	591.9	174.7
11	592.7	203.4
12	593.1	174.6
13	593.6	202.1
14	593.9	195.0
15	595.5	198.1
Range	586.2–595.5	174.6–203.4
Average	591.3	189.9
Uncertainty	-0.86 ~ (+)0.71%	-8.06–7.11%

Notes: 12 or 10 shots whose impact velocities are close to the average value are chosen. The average impact velocity is used in the simulation.

uncertainty study. As shown in the figure, we add two lines to indicate the upper and the lower limits. This means that the bullet impact test data actually show a certain range of uncertainty which, we believe, result mainly from the material irregularity and partially from the impact velocity. We intend to find some correlations such that this measured uncertainty can be predicted numerically with a consideration of a major uncertainty parameter. This will be the topic of the next section.

The test data are first analyzed to estimate how much the uncertainty is. The specific experimental results are included in Table 3, but 10 or 12 shots out of 18 shots are shown in the table. The shots whose impact velocities are close to the average impact velocity are selected. How many shots to be included is arbitrary. It is always true that the more the data you have, the more accurate the range of uncertainty is. The average impact velocity and residual velocity of the selected shots are 412.8 m/s and 221.8 m/s, respectively, for four plies case. The uncertainty in the impact velocity is within  $\pm 1.4\%$ , while that in the residual velocity is within  $\pm 7.6\%$ . This ratio is determined by the difference between the maximum value and the average value normalized by the average value. Even for eight plies case, a similar uncertainty is also estimated and shown in Table 3(b). It can be noted that this average impact velocity will be used as an input in the numerical simulations.

### 3. Numerical Simulations

#### 3.1. *Micro-surrogate model*

For the micro-analysis of heterogeneous materials, the traditional numerical method is to use the representative volume element (RVE). In this work, instead of RVE [Hill, 1963], the unit volume element (UVE) is used. This is mainly because the periodic boundary condition can often be inappropriate for composite plates. The heterogeneous structure model in this research is shown in Fig. 4. Since the details of the modeling methodology are addressed in the paper [Shang *et al.*, 2014], a brief description is provided here. A representative stress value of the UVE is estimated using an average scheme:

$$\sigma = f(\varepsilon, \text{failure}) \quad \bar{\sigma}_{ij} = \frac{1}{V} \int_V \sigma_{ij} dV, \quad (3.1)$$

where  $\sigma_{ij}$  is the local stress in the UVE and  $V$  is the volume.

In order to apply random strain values as inputs for the UVE analysis, Latin hypercube sampling strategy is chosen. Simulations were conducted with the commercial code, Abaqus. All other constraints and boundary conditions are imposed through the python script. From several hundred runs with the strain values as input and stress values as output, a surrogate is constructed for each stress component as

$$\sigma = f(\varepsilon, \text{failure}). \quad (3.2)$$

If we adopt the popular form of Johnson–Cook model [Johnson and Cook, 1985], a strain-rate form is introduced as the second set of brackets. Then, the equation can

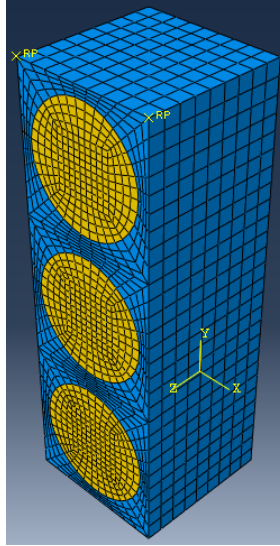


Fig. 4. Heterogeneous structure model of unidirectional fiber-reinforced composites.

be written as

$$\sigma = f(\varepsilon, \text{failure})(1 + C \ln \dot{\varepsilon})(\text{VOF}). \quad (3.3)$$

The data available in the literature show diversity whether the effect of strain rate is important; some fibers are and others not. It can be also said that the effect will not be significant up to certain strain rate. Since this is another challenging subject, the strain rate effect is not considered presently. Note that the fiber volume fraction (VOF), as the third set of brackets, may vary in a linear manner for a small deviation in VOF (less than 10%).

### 3.2. Interface between micro- and macro-model

The built surrogate model is included into the user-subroutine material card MAT45 of LS-DYNA3D. One trivial issue is that the total strain is not available inside the most user-defined material subroutines but the strain increment and the deformation gradient are. Since the surrogate model is generated as a function of strain (Eq. (3.3)), this is normal for some materials, the deformation gradient is used to extract the current strain. Another issue is modeling several plies with different angles assigned. Generally, inside the user-subroutine, all information is defined in a local coordinate. The transformation back to the global system is done outside the subroutine. This is in fact beneficial since the surrogate model itself is built using UVE in a local coordinate.

Verification of this framework is conducted for two problems: one-element tensile test and real ballistic field shot test. An explicit simulation was carried out using

a basic solid element formulation. These are to be described in the following two sections.

### 3.3. Tensile test problem

*Tensile test:* A tensile test was conducted for a four-layered specimen (0/90/90/0) as shown in Fig. 5. A special care was made to control a uniform distribution of the fiber volume content for glass fiber-reinforced laminates which is 56.3%. The constituents of the composite material are E-glass fiber and epoxy resin. Their elastic properties are already listed in Table 1. The length and width of the specimen are 250 mm and 25 mm, respectively. The total thickness is 3.6 mm. Three measurements of width and thickness have been made with an accuracy of 0.01 mm. GFRP tabs with a thickness of 1–2 mm were used for the tests according to DIN EN ISO. The universal testing machine and a precision CCD camera coupled with a computer are used. The data are compared with the numerical predictions in the following section.

*Simulation:* The computational model is shown in Fig. 5(a). The tensile lab test has been compared with two predictions: (1) the user-defined material from the present surrogate modeling and (2) the composite material model MAT22 available already in the code with parameters calculated from the generic homogenization technique (rule of mixture) as

$$E_c = \text{VOF} \times E_f + (1 - \text{VOF}) \times E_m, \tag{3.4}$$

$$\text{VOF} = \frac{V_f}{V_f + V_m}.$$

Here,  $V_f$  and  $V_m$  are the volumes of fiber and matrix, respectively. In general, the input material properties in MAT22 are calculated using the rule of mixture. However, it is known that this is not accurate for transverse direction property. Hence, we used the homogenized properties directly obtained from RVE micro-analysis. Another modeling issue is that in this card, the failure criterion is not the strain-based one, but the stress-based Chang–Chang model. We need the average

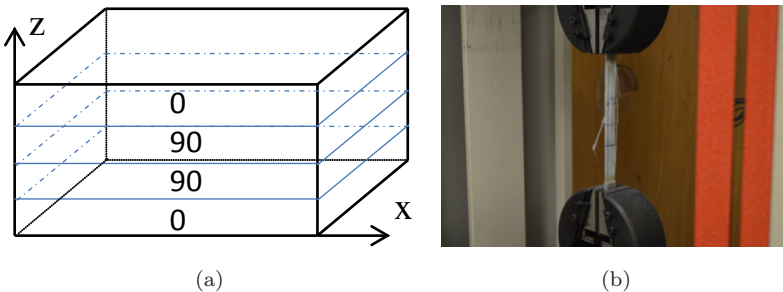


Fig. 5. Unidirectional fiber-reinforced composites: (a) four plies laminates and (b) their tensile test.

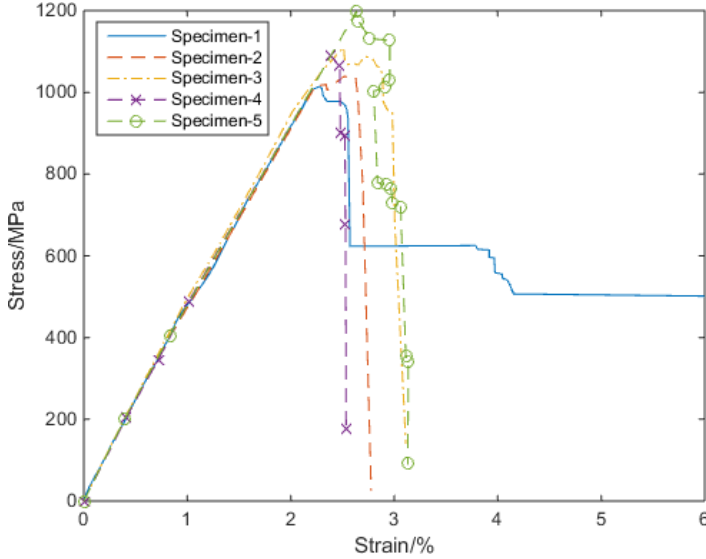


Fig. 6. Tensile test in longitudinal direction.

yield strength. The value of 1.08 GPa which is obtained from several tensile tests is specified. The corresponding failure strain is 2.34%. At the same time, the user-defined subroutine (MAT45) incorporated with the present surrogate model has been tested for two fiber failure strains: minimum (2.26%) and maximum failure strain (2.64%) measured in the tensile test as shown in Fig. 6.

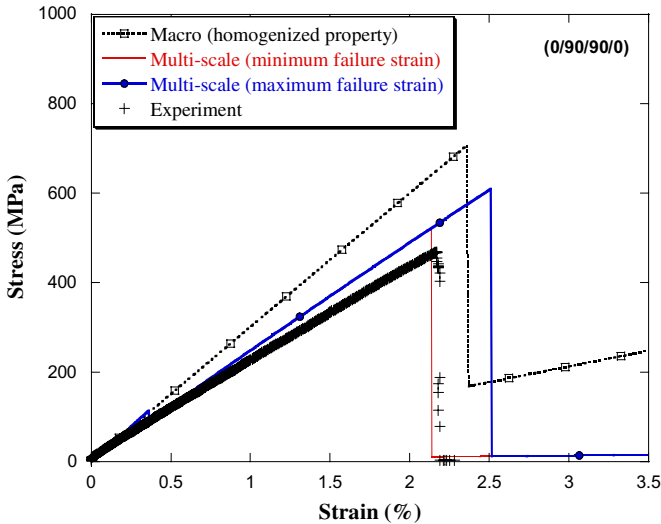


Fig. 7. Comparison of the tensile test for 0/90/90/0 laminates.

Figure 7 shows the stress–strain curves from experiment and simulations. First of all, the slopes of each curve are the same at early-time and start to deviate with the increasing strain. In the macro-MAT22 model, the slope does not change until fiber fails at a strain of around 2.34%. After this point, the material has still some stiffness which is associated with the matrix. The multi-scale model and experiment show a small degradation in slope taking place around a strain of 0.4%. This is attributed to the debonding between fiber and matrix occurring in a 90° ply. For a comparison purpose, two predictions with a maximum failure strain and a minimum failure strain are shown in the figure. The experimental data lie between them. Another thing it can be noted is that a further gradual degradation in slope has been indicated in experiment. This causes a slight difference in the peak stress before a total rupture. Most of all, the experiment and multi-scale model predict almost no residual stress after the major fiber failure, while the macro-analysis using the homogenized property shows significant residual stress.

### 3.4. Ballistic test problem

Now, the impacts onto laminated plates are simulated and the predictions are compared with the ballistic shot data. A three-dimensional computation is conducted. Due to the symmetry, one-quarter domain is used. The domain size is 70 mm (longitudinal) × 50 mm (transverse), which is chosen based on the damage zone area. The bullet is relatively small in dimension compared with the composite plate. So, the total number of element is restricted by the bullet. Five elements are used through the bullet radius direction, and similar element size is used to model the wide plate. The impact velocities as input in simulations are 412.8 m/s for four plies and 591.3 m/s for eight plies laminates, which are the average impact velocities of the test (Table 3).

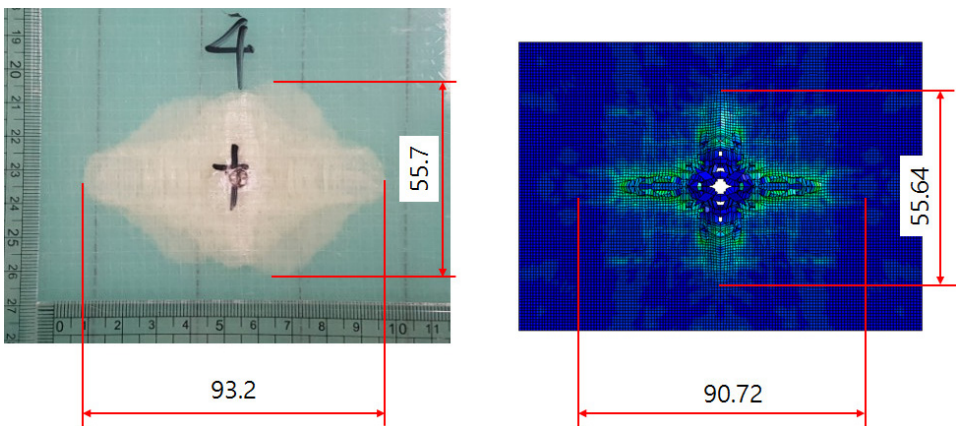


Fig. 8. Photographs of the recovered plates after perforation: (a) experiment and (b) simulation.

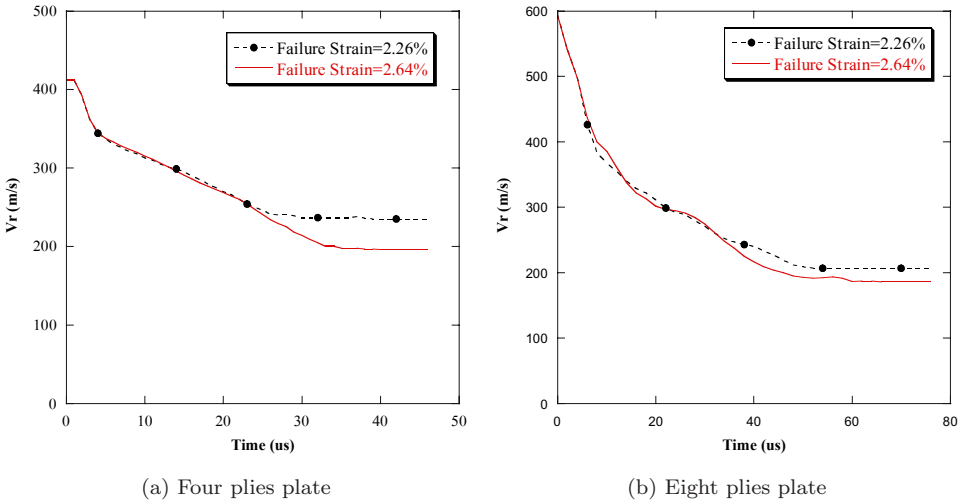


Fig. 9. Time history of bullet penetration velocity moving through (a) four plies plate and (b) eight plies plate.

*Damaged plates:* Figure 8 shows a comparison of the front surfaces of the impacted laminates (four plies) obtained by experiment and simulation. The agreement in the hole diameter and damage pattern is generally excellent.

*Penetration velocities:* The time history of penetration velocity of the bullet moving through the four plies plate is shown in Fig. 9. Two history lines are plotted: one with a failure strain of 2.26% and the other with 2.64% while the impact velocity is the same. As shown in the figure, there is a sudden drop in velocity and followed by a gradual decrease. Up to 25  $\mu\text{s}$  after impact, the penetration velocities are the same for both cases. As can be expected, for the large failure strain case, a complete perforation, where the velocity becomes constant, is further delayed. This results in a reduced residual velocity. A similar trend is also predicted for the case of eight plies plate, but the difference in the final residual velocities is less.

*Residual velocities:* Figure 10(a) shows a comparison of the residual velocity between predictions and test data for the impact onto four plies plate. Two residual velocities are numerically predicted for extreme cases: one with a minimum failure strain and the other with a maximum failure strain. Note that the data are displayed in a normalized scale, indicating more pronounced scatter in the residual velocity than the impact velocity. Zero tolerance in the impact velocity is beyond the current test capability. In general, the two extreme predictions cover the range of uncertainty shown in the test data. The result for the case of eight plies plate is displayed in Fig. 10(b). Again, the simulations are able to predict the residual velocities reasonably well. The lower bound, however, is slightly high such that it does not cover the range of the scattered test data ( $-8 \sim (+)7\%$ ). The upper bound is also higher. The reasons are not clear. It could be that the material strength increases

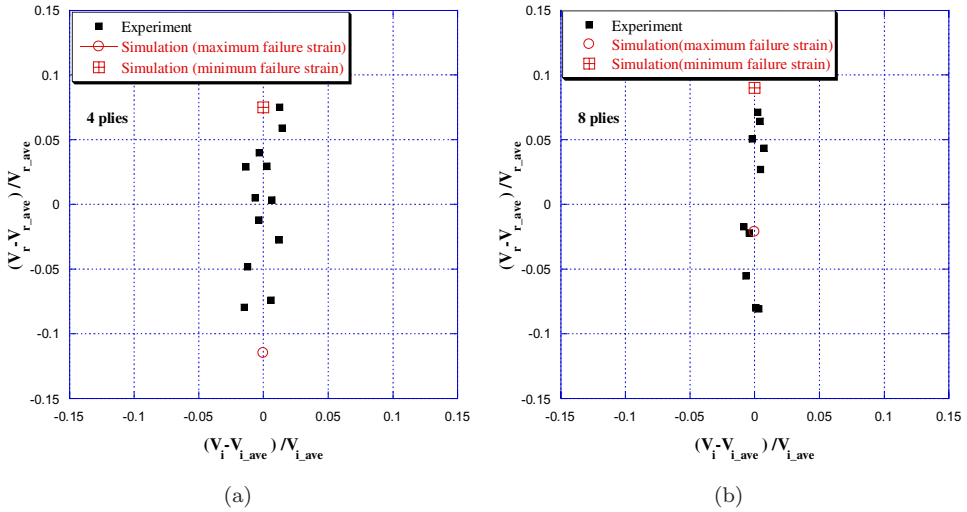


Fig. 10. Comparison of residual velocities between experiment and prediction for (a) four plies plate and (b) eight plies plate.

at a higher impact velocity due to the strain rate effect. Another possibility involves complications associated with the explicit time integration computations.

Most of all, the dominant source of uncertainty in the residual velocity for the perforation onto composite laminates is confirmed to be due to the variation in failure strain, especially for the high-speed ballistic impact problem. The variation in failure strain could be the net outcome associated with several sources of irregularity. This is because the ballistic resistance of fiber composites mostly relies on the fiber tension [Chocron *et al.*, 2013]. Furthermore, since the minimum and maximum failure strains are captured in a ply level tensile test from 10 sets of test, they are entitled to govern the fracture of laminate plates subjected to the high-speed ballistic impact.

#### 4. A Further Discussion on Uncertainty Estimation

Table 4 summarizes the tensile strength and its failure strain which are obtained from 10 trials of tensile test (0° direction, as shown in Fig. 6). The scatter in failure strain is an indication that there is a difference in the ability of energy absorption; thus for the real impact event, some scatter in the residual velocity is also expected. In Table 5, this rational is clearly demonstrated by showing the minimum and maximum values obtained from the ballistic test.

Now, we try to analyze the bullet impact onto composites with the text level energy argument. The data generated in this work can serve as a basis for uncertainty estimation for future comprehensive study. First, energy stored in the target plates is examined. Figure 11(a) shows the stress–strain curve for a brittle material having a certain variation in the failure strain, that is, correspondingly, variation in

Table 4. Tensile strength and the corresponding failure strain from 0° tensile test of unidirectional laminates.

	Min	Average	Max	(Min/Max) <sup>2</sup>
Maximum stress (MPa)	1002	1080	1185	0.715
Failure strain (%)	2.26	2.47	2.64	

Table 5. Measured residual velocities from a bullet impact onto laminates.

	$V_{i\_ave}$ (m/s)	$V_{r\_min}$ (m/s)	$V_{r\_max}$ (m/s)	$(V_{r\_min})^2/(V_{r\_max})^2$
Four plies	412.8	203.8	238.0	0.733
Eight plies	589.8	174.6	203.4	0.737

the maximum stress. Since the energy stored in a stretched fiber is

$$\text{Stored energy} = \frac{\sigma^2}{2E}, \tag{4.1}$$

the ratio of stored energy for two extreme stress values is

$$\text{Ratio of stored energy} = \frac{\sigma_{min}^2}{\sigma_{max}^2} = \frac{1002^2}{1185^2} = 0.715. \tag{4.2}$$

This says that 28.5% difference in energy absorption can be anticipated between two cases. Note that as a first-order estimation, a linear increase in stress with strain up to failure is assumed.

Next, the kinetic energy of a bullet is examined as shown in Fig. 11(b). The residual kinetic energy after perforation is  $1/2 MV_r^2$ . Since the recovered bullet shows almost no deformation in shape, it can be assumed to be a rigid body. Then, the ratio of residual kinetic energy for two extreme cases is

$$\text{Ratio of residual kinetic energy} = \frac{V_{r\_min}^2}{V_{r\_max}^2}. \tag{4.3}$$

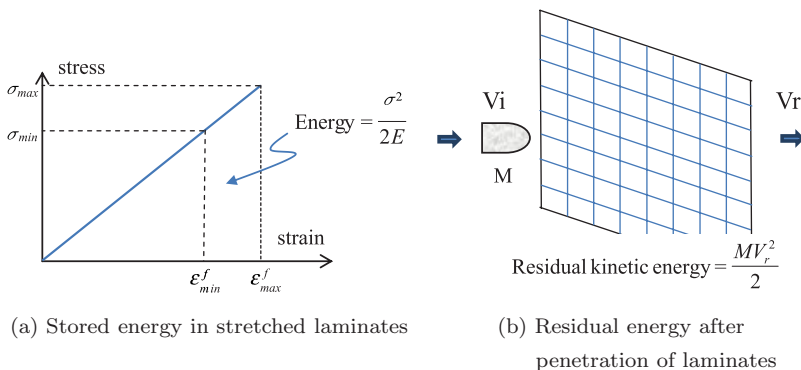


Fig. 11. Energy argument for impact of a bullet onto unidirectional fiber laminates.

Using the measured data in Table 5, this ratio becomes 0.733 for four plies laminates and 0.737 for eight plies laminates, which are very close to the ratio of stored energy 0.715 in Eq. (4.2).

This energy argument here can provide a certain confidence on the correlation between the scattered failure strain data in the tensile test and the scattered residual velocity data in the impact field test data.

## 5. Conclusion

The surrogate-based multi-scale model has been applied to the analysis of ballistic impact of a bullet onto composite laminates, with a special emphasis on the prediction of the uncertainty range shown in the ballistic shot data. From the tensile test using 10 specimens, one source of material uncertainty is identified as the failure strain which ranges from 2.26–2.62%.

The surrogate material model has been integrated into the user-defined subroutine of LS-DYNA in order to simulate the bullet impact onto composite plate. By changing only the value of failure strain, numerical simulations have been demonstrated to be able to predict similar range of uncertainty measured in the test. This is because the resistance primarily comes from the fiber tension. In this study, the bullet impact velocity varies from 400 m/s to 600 m/s, and the obtained range of uncertainty in the residual velocity is  $\pm 7\%$ . This finding can provide some insight for the estimation of the uncertainty in the high-speed ballistic test. Hence, it deserves one step advance in the real design work.

Currently, all the simulations were conducted by using a conventional solid element in the finite element code. The thick shell element already available in the code will also be a good choice for further reduction in the computational time. In the future, it is also necessary to include the strain rate effect to enhance the prediction accuracy.

## Acknowledgment

This work is supported by the Research Program (2014M3C1A9060719).

## References

- Antonio, C. C. and Hoffbauer, L. N. [2008] “From local to global importance measures of uncertainty propagation in composite structures,” *Composite Structures* **87**, 213–225.
- Bandaru, A. K. and Ahmad, S. [2015] “Effect of projectile geometry on the deformation behavior of Kevlar composite armors under ballistic impact,” *International Journal of Applied Mechanics* **7**(3), 1550039.
- Chocron, B., Rodriguez, J. and Galvez, S. [1997] “A simple analytical model to simulate textile fabric ballistic impact behaviors,” *Textile Research Journal* **67**, 520–528.

- Chocron, S., King, N., Bigger, R., Walker, J. D., Heisserer, U. and van der Werff, V. [2013] "Impacts and waves in Dyneema HB80 strips and laminates," *Journal of Applied Mechanics* **80**, 031806.
- Cunniff, P. M. [1992] "An analysis of the system effects in woven fabrics under ballistic impact," *Textile Research Journal* **62**(9), 495–509.
- Grujicic, M., Snipes, J. S. and Chandrasekharan, N. [2013] "A simple model for the prediction of the ballistic limit in thick section composite laminates," *International Journal of Engineering Practical Research* **2**(2), 31–48.
- Hayhurst, C. J., Hiermaier, S. J., Clegg, R. A., Riedel, W. and Lambert, M. [1999] "Development of material models for Nextel and Kevlar-epoxy for high pressures and strain rates," *International Journal of Impact Engineering* **23**, 365–376.
- Hill, R. [1963] "Elastic properties of reinforced solids: Some theoretical principles," *Journal of Mechanics and Physics of Solids* **11**(5), 357–372.
- Johnson, G. R. and Cook, W. H. [1985] "Fracture characteristics of three metals subjected to various strains, strain rates, temperatures and pressures," *Engineering Fracture Mechanics* **21**(1), 31–48.
- Katz, S., Grossman, E., Gouzman, I., Murat, M., Wiesel, E. and Wagner, H. D. [2008] "Response of composite materials to hypervelocity impact," *International Journal of Impact Engineering* **35**(12), 1606–1611.
- Lee, M. [2014] "Optimum thickness ratio of two spaced plate system against hypervelocity impact," *International Journal of Applied Mechanics* **6**(2), 1450018.
- Naik, N. K., Shrirao, P. and Reddy, B. C. K. [2006] "Ballistic impact behavior of woven fabric composites: Formulation," *International Journal of Impact Engineering* **32**, 1521–1552.
- Raguraman, M., Deb, A. and Gupta, N. K. [2010] "Semi-empirical procedures for estimation of residual velocity and ballistic limit for impact of mid steel plates by projectiles," *Latin American Journal of Solids and Structures* **7**, 63–76.
- Ryan, S. and Christiaansen, E. L. [2010] "Micrometeoroid and orbital debris (MMOD) shield ballistic limit analysis program," NASA/RTM-2009-214789, Feb. 2010, National Aeronautics and Space Administration, Johnson Space Center, Houston, TX 77058.
- Ryan, S., Schaefer, F., Destefanis, R. and Lambert, M. [2008] "A ballistic limit equation for hypervelocity impacts on composite honeycomb sandwich panel satellite structures," *Advances in Space Research* **41**(7), 1152–1166.
- Shang, S., Kim, N. H. and Lee, M. [2014] "Integration of multi-scale modeling of composites under high strain rate impact with surrogate," *American Society for Composite 29th Technical Conference*, San Diego, USA, 8–10 Sep.
- Sun, C. T. and Potty, S. V. [1996] "A simple model to predict residual velocities of thick composite laminates subjected to high velocity impact," *International Journal of Impact Engineering* **18**, 339–353.
- Williams, K. V. and Vaziri, R. [2001] "Application of a damage mechanics model for predicting the impact response of composite materials," *Composite Structures* **79**, 997–1011.